Role of the cofilin 2 gene in regulating the myosin heavy chain genes in mouse myoblast C2C12 cells

HONGYAN ZHU[1], HUIXIN YANG[2], SONG ZHAO[3], JUNFENG ZHANG[1], DAN LIU[1], YUMIN TIAN[1], ZHIYI SHEN[1] and YUHONG SU[1]

[1]College of Animal Science and Veterinary Medicine, Jinzhou Medical University, Jinzhou, Liaoning 121001; [2]College of Veterinary Medicine, Nanjing Agricultural University, Nanjing, Jiangsu 210000; [3]Central Laboratary, Jinzhou Medical University, Jinzhou, Liaoning 121001, P.R. China

Received January 21, 2016; Accepted November 15, 2017

DOI: 10.3892/ijmm.2017.3272

Abstract. The cofilin 2 (*CFL2*) and myosin heavy chain (*MyHC*) genes play a key role in muscle development and myofibrillar formation. The aim of the present study was to investigate the effect of *CFL2* on genes involved in fiber formation and the mechanisms underlying this process. Undifferentiated and differentiated C2C12 cells (UDT and DT, respectively) were transfected with *CFL2* small interfering RNA (siRNA). *CFL2* mRNA and protein levels were assessed using reverse transcription polymerase chain reaction (RT-PCR) and western blotting, respectively. *MyHC* gene expression in UDT and signaling pathway-related factors were observed with quantitative PCR (RT-qPCR) and western blotting. Fluorescence microscopy was used to analyze the cytoskeletal effects of *CFL2*. The mRNA and protein expressions of *CFL2*, four *MyHC* isoforms (*MyHC-I*, *MyHC-IIa*, *MyHC-IIb* and *MyHC-IIx*), p38 mitogen-activated protein kinase, cAMP-response element-binding protein, AMP-activated protein kinase α1, and myocyte enhancer factor 2C, were significantly decreased in UDT. However, extracellular signal-regulated kinase 2 expression was significantly increased. Slightly decreased CFL2 protein and mRNA expression was observed in DT C2C12 cells transfected with *CFL2* siRNA. Fluorescence microscopy revealed a significant decrease of *CFL2* in the cytoplasm, but not the nucleus, of UDT, compared with normal cells. These results indicated that the mouse *CFL2* gene may be involved in the regulation of *MyHC* via the key signaling molecules of *CFL2*-related signaling pathways.

Correspondence to: Professor Yuhong Su, College of Animal Science and Veterinary Medicine, Jinzhou Medical University, section 3, 40 Songpo Road, Linghe, Jinzhou, Liaoning 121001, P.R. China
E-mail: suyh652@sina.com

Key words: cofilin 2, gene expression, muscle, myosin heavy chain, mouse, RNA interference

Introduction

The cofilin 2 (*CFL2*) gene plays a key role in muscle development in mammals. CFL plays a crucial role in the regulation of actin by enhancing the turnover of actin filaments (1,2). Mammalian *CFL* occurs as non-muscle type (*CFL1*) or muscle-type (*CFL2*). In embryos, *CFL1* is predominantly expressed in non-myoblast cells. The CFL2 protein appears in skeletal and cardiac myoblasts, particularly in the I bands and Z lines of skeletal myoblasts. During muscle development, *CFL1* expression decreases, while *CFL2* expression increases and eventually becomes predominant in mature mammalian skeletal myoblasts (3). The CFL2 transcript is spliced using either exon1a or exon1b to form the *CFL2a* and *CFL2b* transcripts, respectively. The *CFL2a* transcript is found in various tissues, while the *CFL2b* transcript is mainly found in mature skeletal muscle. CFL binds and polymerizes filamentous F-actin and inhibits the polymerization of monomeric G-actin in a pH-dependent manner, in part through interactions with tropomyosins (4,5).

Four isoforms of myosin heavy chain (*MyHC*) are expressed in skeletal muscle throughout the period of development, and are determinants of muscle development (6): I, slow oxidative; IIa, fast oxidative; IIb, fast glycolytic; and IIx/d, mixed (7). It was previously suggested that *MyHC* composition affects meat quality in livestock (8). Meat characteristics, in particular edibility, may be strongly affected by muscle fiber types, which depend on *MyHC* mRNA expression (8). Indeed, the expression of *MyHC-I* is associated with the pH value of the meat 24 h after death (pH_{24h}) and drip loss (a characteristic of meat that represents its water-retaining capacity), while *MyHC-II* expression is correlated with juiciness, off-flavor, and tenderness of the meat (8). Our previous study demonstrated that *CFL2b* overexpression regulated the fast muscle fiber trait by increasing the expression of *MyHC-IIb* and *-IIx/d* (9). However, the effects on *MyHC* when *CFL2* is disrupted have not been determined.

MyHC and *CFL* expression are associated with four cellular signaling pathways, including AMP-activated protein kinase (AMPK) (10,11), calmodulin (CaM), Rho, and mitogen-activated protein kinase (MAPK) (12-14). Five important proteins in these pathways, including extracellular

signal-regulated kinase 2 (ERK2) (15), p38 MAPK (16), myocyte enhancer factor 2C (MEF2C) (17,18), cAMP-response element-binding protein (CBP) (16) and AMPKα1 (19), may affect the expression of *MyHC* after inhibiting *CFL2* expression.

To identify the involvement of *CFL2* in skeletal muscle and the period during which *CFL2* exerts its effects, the present study investigated the effects of *CFL2* on actin fibers by studying the *CFL2* and *MyHC* genes in undifferentiated and differentiated C2C12 cells transfected with the *CFL2* siRNA. In addition, the protein expression of pathway-related genes, including ERK2, p38 MAPK, MEF2C, CBP and AMPKα1, was determined.

Materials and methods

Cell culture and transfection. Mouse C2C12 myoblasts (GNM26) obtained from the Cell Bank of the Chinese Academy of Sciences (Shanghai, China) were grown in Dulbecco's modified Eagle's medium (DMEM) supplemented with 10% (v/v) fetal calf serum (both from Invitrogen; Thermo Fisher Scientific, Carlsbad, CA, USA) at 37˚C with 5% CO_2 in humidified chambers. Differentiation of C2C12 cells was induced by replacing the medium with 2% horse serum for 6 days.

Cells in 6-well plates were transfected with *CFL2* small interfering RNA (siRNA) using the liposome method (FuGene HD transfection reagent; Roche, Shanghai, China) when they reached 50% confluence, according to the manufacturer's instructions (9). The RNA interfering effects of siRNAs were confirmed by western blotting and reverse transcription-quantitative polymerase chain reaction (RT-qPCR). The undifferentiated cells were then screened with 500 μg/ml of G418 (Roche) to obtain single cell clones.

siRNA for CFL2 gene. Two siRNA pairs (*CFL2*-1 and *CFL2*-2; Table I) were selected for targeting the murine *CFL2* gene (NM_007688) using a web-based siRNA design application (http://sirna.wi.mit.edu/home.php) (20). The selected siRNA pairs were then synthesized by Genechem (Shanghai, China). Undifferentiated cells were transfected with siRNA concentrations of 50, 100 and 150 nmol/l of *CFL2*-1, and 50 and 100 nmol/l of *CFL2*-2. Cells transfected with scramble siRNA were used as controls. The effects of *CFL2* siRNA were identified by RT-PCR and western blotting.

Experimental groups. Cells were divided into the following groups: Undifferentiated, C2C12 cells transfected with scramble siRNA (UDN); undifferentiated, C2C12 cells transiently transfected with *CFL2* siRNA (UDT); differentiated, C2C12 cells transfected with scramble siRNA (DN); and differentiated, C2C12 cells transiently transfected with *CFL2* siRNA (DT).

RT-PCR. RNA was extracted from C2C12 cells using an RNeasy mini kit (Qiagen, Hilden, Germany), and first-strand cDNA was synthesized from purified total RNA with a reverse transcription kit (Takara, Dalian, China). RT-PCR was performed according to standard protocols using the primers indicated in Table II. The final volumes of each reaction were 20 μl, including 10 pmol primers, 2 mM $MgCl_2$, 2.5 mM dNTP, and 1 U TaqDNA polymerase (Takara). The samples underwent PCR as follows: Denaturation for 5 min at 94˚C; 30 cycles of 30 sec at 94˚C, 30 sec at 56.7˚C, and 45 sec at 72˚C; and extension for 10 min at 72˚C. Following amplification, 10 μl PCR product was analyzed using 1% agarose gel electrophoresis and visualized using ethidium bromide and UV light.

RT-qPCR. RT-qPCR was performed to detect mRNA expression of *MyHC-I*, *MyHC-IIa*, *MyHC-IIb*, *MyHC-IIx* and glyceraldehyde 3-phosphate dehydrogenase (*GAPDH*) in UDN, UDT, DN and DT. The cDNA template was prepared from mRNA directly harvested from *CFL2*-transfected cells at $1x10^6$ cells/well. First-strand reverse transcription was performed using 100 ng total RNA with a reverse transcription kit (Takara); the RT-qPCR primers were also from Takara (Table III). SYBR-Green RT-qPCR assay for the target genes was performed in optical 96-well plates using the SYBR® Premix EX Taq™ II (DRR081A; Takara) and the 7500 Fast Real-Time PCR system (Applied Biosystems, Foster City, MA, USA), according to the manufacturer's instructions. Results were detected quantitatively in real-time by relative quantitation of two standard curves. The process consisted of 41 cycles, including 1 cycle of 10 sec at 95˚C and 40 cycles of 5 sec at 95˚C and 20 sec at 60˚C. All experiments were performed three times, each time in triplicate.

Table I. siRNA sequences for the target sites in the *CFL2* gene.

siRNA	Primer sequences (5'-3')	Target site
CFL2-1	F: CUGAAAGUGCACCGUUAAAdTdT	315-337
	R: UUUAACGGUGCACUUUCAGdTdT	
CFL2-2	F: GCUCUAAAGAUGCCAUUAAdTdT	354-376
	R: UUAAUGGCAUCUUUAGAGCdTdT	
Scramble	CTTGAAGGAAAGCCACTAT	-

CFL2, cofilin 2; F, forward primer; R, reverse primer.

Table II. RT-PCR primers for the target genes.

Target genes	Primer sequences (5'-3')	PCR product size
CFL2	F: ATCTTGGTGGGTGACATTGG	322 bp
	R: CAAGGGAAACTACAACACTGC	
GAPDH[a]	F: GCAGTGGCAAAGTGGAGATT	790 bp
	R: TGAAGTCGCAGGAGACAACC	
GAPDH[b]	F: GCGAGACCCCACTAACATC	171 bp
	R: TTCACACCCATCACAAACA	

[a]Primer of *GAPDH* used in Fig. 1A. [b]Primer of *GAPDH* used in Fig.2A. RT-PCR, reverse transcription-polymerase chain reaction; CFL2, cofilin 2; GAPDH, glyceraldehyde 3-phosphate dehydrogenase; F, forward primer; R, reverse primer.

Table III. Oligonucleotide primers for RT-qPCR.

Genes	Primer sequences (5'-3')	PCR product size
MyHC-I	F: ATGAGCTGGAGGCTGAGCA R: TGCAGCCGCAGTAGGTTCTT	124 bp
MyHC-IIa	F: ATTCTCAGGCTTCAGGATTTGGTG R: CTTGCGGAACTTGGATAGATTTGTG	114 bp
MyHC-IIb	F: GAGTTCATTGACTTCGGGATGG R: TGCTGCTCATACAGCTTGTTCTTG	143 bp
MyHC-IIx	F: AAGGGTCTGCGCAAACATGA R: TTGGCCAGGTTGACATTGGA	173 bp
GAPDH	F: GCGAGACCCCACTAACATC R: TTCACACCCATCACAAACA	171 bp

RT-qPCR, reverse transcription-quantitative polymerase chain reaction; GAPDH, glyceraldehyde 3-phosphate dehydrogenase; MyHC, myosin heavy chain; F, forward primer; R, reverse primer.

Western blotting. Western blotting for CFL2, p38, ERK2, CBP, AMPKα1, MEF2C and GAPDH was performed in UDN and UDT. The cells were washed, harvested, lysed with a lysis buffer [20 mM Tris-Cl, pH 7.5, 150 mM NaCl, 1% sodium dodecyl sulfate (SDS), 1% Triton X-100, 10 μg/ml leupeptin, 1 mM aprotinin and 1 mM phenylmethanesulfonyl fluoride] on ice for 30 min, and centrifuged at 14,000 x g at 4˚C for 15 min. Proteins were resolved by SDS-polyacrylamide gel electrophoresis, transferred onto polyvinylidene difluoride membranes, blocked at room temperature for 1 h in 5% bovine serum albumin (BSA), and then incubated overnight at 4˚C on a rotator with the primary antibodies: CFL2 (1:1,000; goat, SAB2500255; Sigma-Aldrich; Merck KGaA, St. Louis, MO, USA), p38 (1:1,000; mouse, ab31828), ERK2 (1:1,000; rabbit, ab32081), CBP (1:1,000; mouse, ab50702), AMPKα1 (1:1,000; mouse, ab80039) (all from Abcam, Cambridge, MA, USA), MEF2C (1:1,000; rabbit, SAB2103534; Sigma-Aldrich; Merck KGaA) and GAPDH (1:2,000; mouse, ab8245; Abcam). The membranes were washed four times with TBST and incubated for 1 h with an appropriate horseradish peroxidase (HRP)-conjugated secondary antibody (1:3,000). Immunoreactivity was visualized with an enhanced chemiluminescence detection reagent (ECL; Pierce, Rockford, IL, USA). All the experiments were performed three times, each time in triplicate.

CFL2 and F-actin analysis by fluorescence microscopy. *CFL2* siRNA was transfected into cells. *CFL2* and F-actin were labeled with fluorescein isothiocyanate (FITC) and tetramethylrhodamine (TRITC)-labeled phalloidin (Sigma-Aldrich; Merck KGaA) to differentiate between UDN and UDT. In terms of TRITC-labeled phalloidin methodology, UDN and UDT were grown on glass coverslips until they reached the logarithmic growth stage. Specimens were then washed three times in phosphate-buffered saline (PBS) and fixed with 4% paraformaldehyde at room temperature for 30 min. After washing three times with PBS, the specimens were permeabilized with 0.2% Triton X-100 for 10 min, washed three times with PBS, and blocked with 1% BSA for 30 min. The coverslips were incubated for 10 min with diluted phalloidin (1:200, protected from light) and washed three times in PBS. The coverslips were mounted and observed with 90% glycerol in PBS. Notably, the FITC methodology is equivalent to the TRITC-labeled phalloidin approach, but additionally requires an overnight antibody incubation step prior to hybridization with diluted FITC (1:100, protected from light). UDN were used as controls. The cells were examined using a Zeiss epifluorescence microscope (Carl Zeiss AG, Oberkochen, Germany), as described in Table IV.

Table IV. Fluorescent staining of *CFL2* and F-actin in C2C12 cells.

CFL2 expression levels	Fluorescent staining method	
	CFL2	F-actin
Low	IgG antibody labeling with FITC	TRITC-labeled phalloidin
Normal	IgG antibody labeling with FITC	TRITC-labeled phalloidin

CFL2, cofilin 2; Ig, immunoglobulin; FITC, fluorescein isothiocyanate; TRITC, tetramethylrhodamine.

Statistical analyses. The results were analyzed using SPSS 17.0 software (IBM, Armonk, NY, USA). Data are presented as means ± standard deviation. Experimental and control groups were compared using analysis of variance followed by Least Significant Difference post hoc analysis. P-values <0.05 were considered to indicate statistically significant differences.

Results

Knockdown of CFL2 by CFL2 siRNA. We first validated the RNA interference (RNAi) effects of *CFL2* siRNAs. RT-PCR amplification of *CFL2* and *GAPDH* was analyzed (Fig. 1A). The results revealed that CFL2-1 siRNA at 50 nM exerted the strongest inhibitory effect of all five experimental groups (P<0.05; Fig. 1B), whereas, as expected, the scramble siRNA exerted no effect on *CFL2* expression. The results of western blotting were consistent with the RT-PCR results (Fig. 1C and D). Therefore, the most effective siRNA sequence for *CFL2* was *CFL2*-1 siRNA at a concentration of 50 nM.

MyHC expression is downregulated in undifferentiated C2C12 cells treated with CFL2 RNAi. RNAi significantly inhibited *CFL2* in undifferentiated cells (P<0.05) and in DT compared with DN (P<0.05; Fig. 2A and B). Therefore, regardless of cellular differentiation, RNAi significantly inhibited *CFL2* mRNA expression in C2C12 cells. Western blot analyses were also consistent with the RT-PCR results (P<0.05; Fig. 2C and D).

RT-qPCR amplification was used to determine the expression of *MyHC* genes in differentiated and undifferentiated

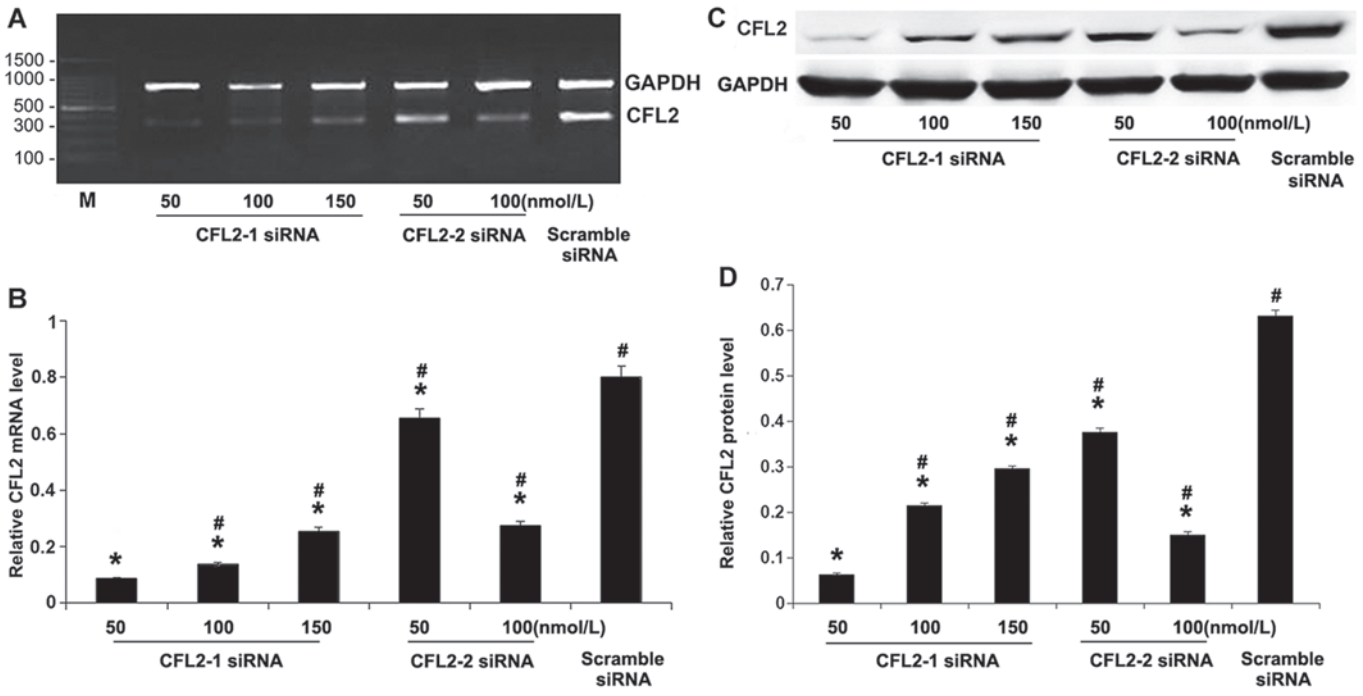

Figure 1. Cofilin 2 (*CFL2*) mRNA and protein expression in C2C12 cells transfected with *CFL2* siRNA. (A) Representative image of RT-PCR. (B) Statistical data of (A). (C) Representative image of western blotting. (D) Statistical data of (C). The histogram shows the results as mean ± standard deviation of three experiments performed in triplicate. Expression was normalized to glyceraldehyde 3-phosphate dehydrogenase (GAPDH). M, 100 bp standard marker. *P<0.05 vs. scramble siRNA group; #P<0.05 vs. CLF2-1 siRNA 50 nmol/l. siRNA, small interfering RNA; RT-PCR, reverse transcription-polymerase chain reaction.

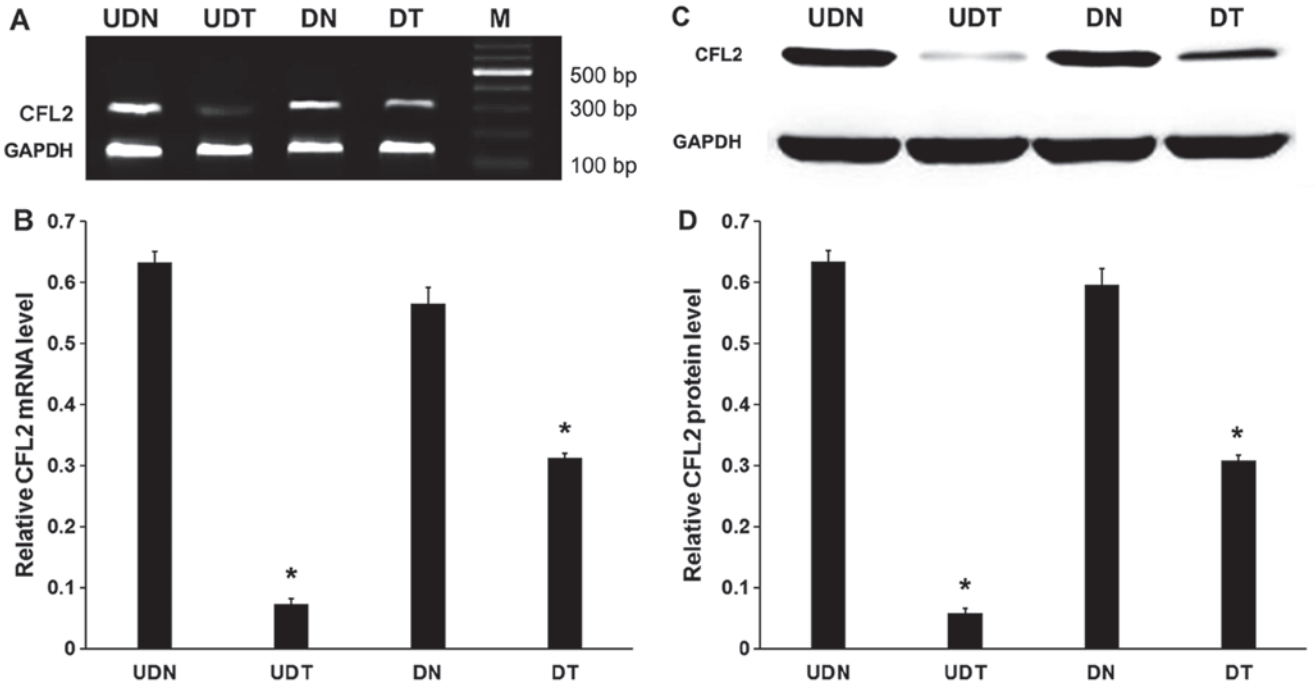

Figure 2. Cofilin 2 (*CFL2*) mRNA and protein expression after RNAi in undifferentiated and differentiated C2C12 cells. (A) Representative image of RT-PCR of *CFL2* and glyceraldehyde 3-phosphate dehydrogenase (*GAPDH*). M, 100 bp standard marker. (B) Statistical data. *GAPDH* was used as an internal control. (C) Representative image of western blotting of CFL2 and GAPDH. (D) Statistical data. GAPDH was used as an internal control. All experiments were performed three times, each time in triplicate. *P<0.05 UDT vs. UDN and DT vs. DN. UDN, undifferentiated C2C12 cells transfected with scramble siRNA; UDT, undifferentiated C2C12 cells transiently transfected with CFL2 siRNA; DN, differentiated C2C12 cells transfected with scramble siRNA; DT, differentiated C2C12 cells transiently transfected with CFL2 siRNA.

C2C12 cells following *CFL2* siRNA transfection. The *MyHC*/*GAPDH* expression in undifferentiated and differentiated cells is shown in Fig. 3. *MyHC-I*, *MyHC-IIa*, *MyHC-IIb* and *MyHC-IIx* gene expressions were significantly decreased in UDT (P<0.05).

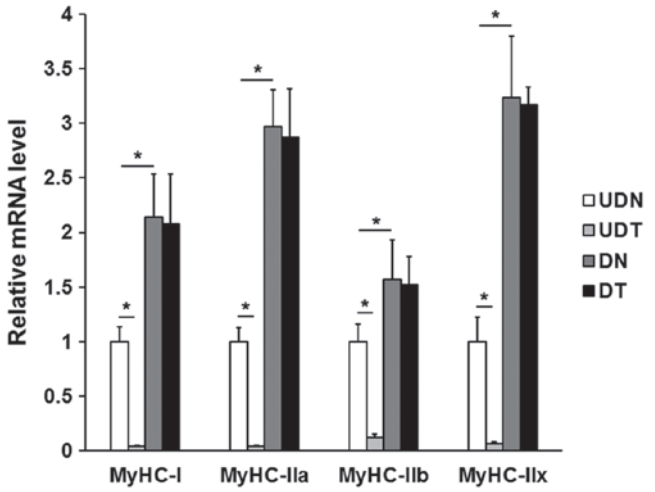

Figure 3. Myosin heavy chain (*MyHC*) mRNA expression with cofilin 2 (*CFL2*) RNAi in differentiated and undifferentiated C2C12 cells, using RT-qPCR. Glyceraldehyde 3-phosphate dehydrogenase (GAPDH) was used as an internal control. The level of mRNA in the UDN group was set as 1 and the other groups were normalized to UDN. All experiments were performed three times, each time in triplicate. **P<0.01. RT-qPCR, reverse transcription-quantitative polymerase chain reaction; UDN, undifferentiated C2C12 cells transfected with scramble siRNA; UDT, undifferentiated C2C12 cells transiently transfected with CFL2 siRNA; DN, differentiated C2C12 cells transfected with scramble siRNA; DT, differentiated C2C12 cells transiently transfected with CFL2 siRNA.

However, in DT, RNAi had almost no effect on *MyHC* expression, suggesting that *MyHC* expression is generally proportional to that of *CFL2* prior to differentiation of cells into muscle fibers. These results suggest that *MyHC* mRNA expression was elevated after differentiation (P<0.05), and that *MyHC* genes were not significantly affected by downregulation of *CFL2* only in undifferentiated cells. With this in mind, subsequent experiments were only performed in the UDT and UDN groups.

Muscle fiber signaling pathway-related factors are altered by CFL2 RNAi in undifferentiated C2C12 cells. The expression of key signaling molecules in the AMPK, CaM, Rho and MAPK pathways (including p38 MAPK, ERK2, CBP, AMPKα1 and MEF2C) was measured by western blotting. The expressions of p38 MAPK, CBP, AMPKα1 and MEF2C proteins were significantly decreased in UDT (P<0.05). By contrast, ERK2 protein expression was significantly increased compared with UDN (P<0.05; Fig. 4).

CFL2 alters F-actin formulation in C2C12 cells. In UDN, *CFL2* (green fluorescence) was diffusely distributed in the cytoplasm and nucleus of the cells (Fig. 5A). UDT exhibited a similar diffuse *CFL2* distribution pattern (Fig. 5B).

F-actin structures were not significantly different in UDT compared to UDN with *CFL2* expression. The F-actin bundles, however, exhibited a tendency to form amorphous diffuse patterns (Fig. 5C and D).

Discussion

The aim of the present study was to demonstrate the effects of the mouse myosin-binding protein CFL2 on the expression of *MyHC*, which may play a pivotal role in the cytoskeleton in undifferentiated C2C12 cells. The functions of *CFL2* in undifferentiated and differentiated C2C12 cells were investigated and the results suggested that, in undifferentiated cells, the expression of *MyHC* genes decreased significantly after *CFL2* RNAi; however, there was no obvious change in differentiated cells.

Effects of CFL2 on muscle fiber types. Four *MyHC* isoforms (I, IIa, IIx and IIb) are expressed in adult skeletal muscles (6). *MyHCs* are the primary molecular markers for distinguishing muscle fiber types and studying their characteristics. When *CFL2* gene expression in C2C12 myoblasts is suppressed, the expression of *MyHC-I*, *MyHC-IIa*, *MyHC-IIb* and *MyHC-IIx* is significantly downregulated.

In addition, 6 days after C2C12 differentiation was induced using 2% horse serum, the *CFL2* mRNA and protein expressions in DN were not significantly different from those in undifferentiated cells. The expression of *MyHC-I*, *MyHC-IIa*, *MyHC-IIb* and *MyHC-IIx* increased, indicating that *MyHC* is associated with myoblast differentiation. However, RNAi no longer affected the types of *MyHC*. This may indicate that interactions between *CFL2* and *MyHCs* only occur in undifferentiated cells.

Molecular mechanisms of MyHC in C2C12 cells and CFL2 involvement. Within the four key cellular signaling pathways involved in muscle fiber regulation, there are five important signaling factors: p38 MAPK, ERK2, CBP, MEF2C and AMPKα1. The fast muscle fibers (*MyHC-IIb*/*IIx*) are preferentially affected by MAPK signaling. The dual-specific mitogen-activated protein kinase kinase 3 (MKK3) and the constitutively active MKK6 mutant upstream of p38 MAPK are involved in the maintenance of the fast muscle fiber phenotype (21); they may also be involved in the regulation of *MyHC-IIx* promoter activity in myotubes (12,22). The ERK pathway is also a major pathway that affects fast fibers, as demonstrated by increased *MyHC-IIx* and *MyHC-IIb* transcripts and decreased *MyHC-I* expression following ablation of the ERK1/2 pathway in cultured rat fetal myocytes (23). This mechanism is also consistent with the downregulation of *CFL2* genes as a means to decrease p38 MAPK, *MyHC-IIb* and *MyHC-IIx* expression and to increase ERK2 expression.

It was previously reported that ERK1/2 activity is more than 2-fold higher in fast muscle fibers compared with that in slow muscle fibers (15), suggesting that the ERK1/2 pathway may play a key role in maintaining the fast fiber phenotype. When p38 MAPK activity is inhibited, the promoter activities of fast-type *MyHC-IIb* and *MyHC-IIx* are downregulated. Moreover, p38α/β MAPK is known to mediate *MyHC-IIb* and *MyHC-IIx* expression via CBP and the *MEF2C*/*D* heterodimer (16). When combined with other transcriptional factors (17), *MEF2C* may affect *MyHC* isoform expression in mouse skeletal muscle (18). These prior findings are highly consistent with the results of the present study, in which *MEF2C* and *CBP* expression was decreased by *CFL2* RNAi. Furthermore, a decrease in *MEF2C* expression has been associated with a decrease in *MyHC-I* muscle fibers (24). Expression of the *MEF2C* subunits may also be involved in activation of the p38 MAPK pathway. Thus, *MEF2C* and p38 synergistically regulate and promote type I muscle fibers.

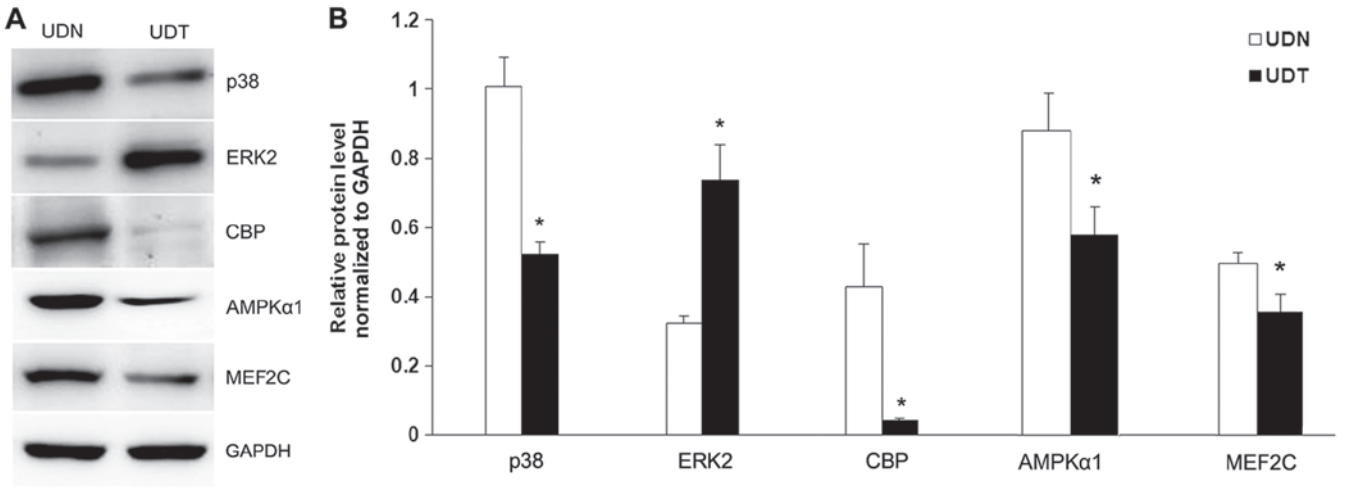

Figure 4. p38, ERK2, CBP, AMPKα1 and MEF2C protein expression in UDN and UDT. (A) Representative image of western blotting of p38, ERK2, CBP, AMPKα1 and MEF2C protein expression in UDN and UDT. (B) Statistical data. Glyceraldehyde 3-phosphate dehydrogenase (GAPDH) was used as an internal control. All experiments were performed three times, each time in triplicate. *P<0.05 vs. UDN. UDN, undifferentiated C2C12 cells transfected with scramble siRNA; UDT, undifferentiated C2C12 cells transiently transfected with CFL2 siRNA; ERK2, extracellular signal-regulated kinase 2; CBP, cAMP-response element-binding protein; AMPK, AMP-activated protein kinase; MEF2C, myocyte enhancer factor 2C.

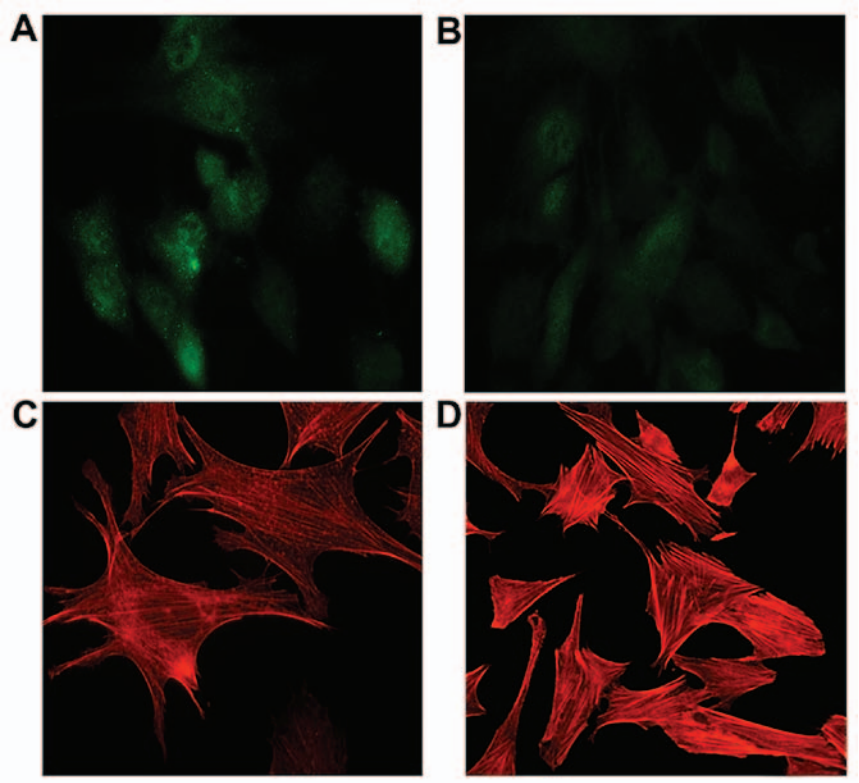

Figure 5. Cofilin 2 (*CFL2*) and F-actin localization in C2C12 cells. (A and B) CFL2 expression and distribution pattern in UDN and UDT (magnification, x200). (C and D) F-actin expression and distribution pattern in UDN and UDT (magnification, x200). UDN, undifferentiated C2C12 cells transfected with scramble siRNA; UDT, undifferentiated C2C12 cells transiently transfected with CFL2 siRNA.

Previously, the authors observed that skeletal muscle in wild-type mice commonly undergoes an AMPK-mediated shift from *MyHC-IIb* to *MyHC-IIa* and *MyHC-IIx* during exercise training (10). These prior results indicated that *AMPKα1* and *AMPKα2* may also alter skeletal muscle composition. This is consistent with the present results, which demonstrated down-regulation of *AMPKα1*, *MyHC-IIa*, *MyHC-IIb* and *MyHC-IIx* following *CFL2* RNAi.

Notably, *MyHC* gene expression was altered in UDT due to RNAi, resulting in downregulation of *MyHC-I*, *MyHC-IIa*, *MyHC-IIb* and *MyHC-IIx* expression. Glycolytic fibers (*MyHC-IIb*) are the most common among these four muscle fiber types. According to the *MyHC* conversion rules (25-27), *MyHC-I* primarily transforms into *MyHC-IIa*. Additional studies are required to confirm the findings of the present study, in part owing to the complexity of *MyHC* conversion due

to overlapping signaling pathways. Additionally, the *MyHC* isoforms that play a key role in the regulation of fast fibers may play a less important role in the regulation of slow fibers under certain physiological conditions. Although *MyHC-I* expression was also found to be decreased in the present study, other isoforms may be able to convert *MyHCs*. Future studies are required to elucidate these isoforms and their roles in the mechanism of *MyHC* conversion.

In conclusion, the findings of the present study indicate that mouse *CFL2* may regulate *MyHC*. In addition, the expression of four *MyHC* isoforms in undifferentiated cells with *CFL2* RNAi was found to be significantly decreased compared with that in differentiated cells. However, further investigations on the exact association of *CFL2* with signaling pathway-related factors are required to fully elucidate the role of *CFL2* in the regulation of *MyHC*.

Acknowledgements

The present study was supported by the National Natural Science Foundations of China (grant no. 31272415/C170102), the Natural Science Foundations of Liaoning Province (grant no. 2015020765) and the Training Programs of Innovation and Entrepreneurship for Undergraduates of Liaoning Province (grant no. 201610160051).

References

1. Chhabra D and dos Remedios CG: Cofilin, actin and their complex observed in vivo using fluorescence resonance energy transfer. Biophys J 89: 1902-1908, 2005.
2. Papalouka V, Arvanitis DA, Vafiadaki E, Mavroidis M, Papadodima SA, Spiliopoulou CA, Kremastinos DT, Kranias EG and Sanoudou D: Muscle LIM protein interacts with cofilin 2 and regulates F-actin dynamics in cardiac and skeletal muscle. Mol Cell Biol 29: 6046-6058, 2009.
3. Mohri K, Takano-Ohmuro H, Nakashima H, Hayakawa K, Endo T, Hanaoka K and Obinata T: Expression of cofilin isoforms during development of mouse striated muscles. J Muscle Res Cell Motil 21: 49-57, 2000.
4. Gillett GT, Fox MF, Rowe PS, Casimir CM and Povey S: Mapping of human non-muscle type cofilin (CFL1) to chromosome 11q13 and muscle-type cofilin (CFL2) to chromosome 14. Ann Hum Genet 60: 201-211, 1996.
5. Ono S and Ono K: Tropomyosin inhibits ADF/cofilin-dependent actin filament dynamics. J Cell Biol 156: 1065-1076, 2002.
6. Asaduzzaman M, Kinoshita S, Siddique BS, Asakawa S and Watabe S: Multiple cis-elements in the 5'-flanking region of embryonic/larval fast-type of the myosin heavy chain gene of torafugu, MYH(M743-2), function in the transcriptional regulation of its expression. Gene 489: 41-54, 2011.
7. Solomon MB, West RL and Carpenter JW: Fiber types in the longissimus muscle from water buffalo and selected domestic beef breeds. Meat Sci 13: 129-135, 1985.
8. Kang YK, Choi YM, Lee SH, Choe JH, Hong KC and Kim BC: Effects of myosin heavy chain isoforms on meat quality, fatty acid composition, and sensory evaluation in Berkshire pigs. Meat Sci 89: 384-389, 2011.
9. Zhao W, Su YH, Su RJ, Ba CF, Zeng RX and Song HJ: The full length cloning of a novel porcine gene CFL2b and its influence on the MyHC expression. Mol Biol Rep 36: 2191-2199, 2009.
10. Röckl KS, Hirshman MF, Brandauer J, Fujii N, Witters LA and Goodyear LJ: Skeletal muscle adaptation to exercise training: AMP-activated protein kinase mediates muscle fiber type shift. Diabetes 56: 2062-2069, 2007.
11. Miranda L, Carpentier S, Platek A, Hussain N, Gueuning MA, Vertommen D, Ozkan Y, Sid B, Hue L, Courtoy PJ, *et al*: AMP-activated protein kinase induces actin cytoskeleton reorganization in epithelial cells. Biochem Biophys Res Commun 396: 656-661, 2010.
12. Long YC, Widegren U and Zierath JR: Exercise-induced mitogen-activated protein kinase signalling in skeletal muscle. Proc Nutr Soc 63: 227-232, 2004.
13. Madak-Erdogan Z, Ventrella R, Petry L and Katzenellenbogen BS: Novel roles for ERK5 and cofilin as critical mediators linking ERα-driven transcription, actin reorganization, and invasiveness in breast cancer. Mol Cancer Res 12: 714-727, 2014.
14. Won KJ, Park SH, Park T, Lee CK, Lee HM, Choi WS, Kim SJ, Park PJ, Jang HK, Kim SH, *et al*: Cofilin phosphorylation mediates proliferation in response to platelet-derived growth factor-BB in rat aortic smooth muscle cells. J Pharmacol Sci 108: 372-379, 2008.
15. Yang SH, Sharrocks AD and Whitmarsh AJ: MAP kinase signalling cascades and transcriptional regulation. Gene 513: 1-13, 2013.
16. Meissner JD, Chang KC, Kubis HP, Nebreda AR, Gros G and Scheibe RJ: The p38alpha/beta mitogen-activated protein kinases mediate recruitment of CREB-binding protein to preserve fast myosin heavy chain IId/x gene activity in myotubes. J Biol Chem 282: 7265-7275, 2007.
17. Al Madhoun AS, Mehta V, Li G, Figeys D, Wiper-Bergeron N and Skerjanc IS: Skeletal myosin light chain kinase regulates skeletal myogenesis by phosphorylation of MEF2C. EMBO J 30: 2477-2489, 2011.
18. Lu J, McKinsey TA, Nicol RL and Olson EN: Signal-dependent activation of the MEF2 transcription factor by dissociation from histone deacetylases. Proc Natl Acad Sci USA 97: 4070-4075, 2000.
19. Wright DC, Hucker KA, Holloszy JO and Han DH: Ca^{2+} and AMPK both mediate stimulation of glucose transport by muscle contractions. Diabetes 53: 330-335, 2004.
20. Reynolds A, Leake D, Boese Q, Scaringe S, Marshall WS and Khvorova A: Rational siRNA design for RNA interference. Nat Biotechnol 22: 326-330, 2004.
21. Delling U, Tureckova J, Lim HW, De Windt LJ, Rotwein P and Molkentin JD: A calcineurin-NFATc3-dependent pathway regulates skeletal muscle differentiation and slow myosin heavy-chain expression. Mol Cell Biol 20: 6600-6611, 2000.
22. Kramer HF and Goodyear LJ: Exercise, MAPK, and NF-kappaB signaling in skeletal muscle. J Appl Physiol (1985) 103: 388-395, 2007.
23. Shi H, Scheffler JM, Pleitner JM, Zeng C, Park S, Hannon KM, Grant AL and Gerrard DE: Modulation of skeletal muscle fiber type by mitogen-activated protein kinase signaling. FASEB J 22: 2990-3000, 2008.
24. Bassel-Duby R and Olson EN: Signaling pathways in skeletal muscle remodeling. Annu Rev Biochem 75: 19-37, 2006.
25. Weiss A, McDonough D, Wertman B, Acakpo-Satchivi L, Montgomery K, Kucherlapati R, Leinwand L and Krauter K: Organization of human and mouse skeletal myosin heavy chain gene clusters is highly conserved. Proc Natl Acad Sci USA 96: 2958-2963, 1999.
26. Whitmer JD, Koslovsky JS, Bähler M and Mercer JA: Chromosomal location of three unconventional myosin heavy chain genes in the mouse. Genomics 38: 235-237, 1996.
27. Knotts S, Rindt H, Neumann J and Robbins J: In vivo regulation of the mouse beta myosin heavy chain gene. J Biol Chem 269: 31275-31282, 1994.